Rheological and Isothermal Crystallization Characteristics of Neat and Calcium Carbonate-Filled Syndiotactic Polypropylene

Pitt Supaphol, Wipasiri Harnsiri

The Petroleum and Petrochemical College, Chulalongkorn University, Pathumwan, Bangkok 10330, Thailand

Received 8 March 2005; accepted 14 June 2005
DOI 10.1002/app.22451
Published online in Wiley InterScience (www.interscience.wiley.com).

ABSTRACT: Steady-state and oscillatory shear behavior of three neat syndiotactic polypropylene (s-PP) resins and a s-PP resin (s-PP#8) filled with $CaCO_3$ particles of varying content, size, and type of surface modification were investigated. All of the neat s-PP resins investigated exhibited the expected shear-thinning behavior. Both the storage and loss moduli increased with decreasing temperature. The shift factors used to construct the master curves were fitted well with both the Arrhenius and the Williams–Landel–Ferry (WLF) equations. The inclusion of $CaCO_3$ particles of varying content, size, and type of surface modification, to a large extent, affected both the steady-state and oscillatory shear behavior of s-PP/$CaCO_3$ compounds, with the property values being found to increase with increasing content, decreasing size, and surface coating of the $CaCO_3$ particles. Lastly, the effects of melt-annealing and crystallization temperatures on isothermal crystallization behavior of s-PP#8 filled with $CaCO_3$ particles of varying content, size, and type of surface modification were also investigated. The half-time of crystallization of neat s-PP#8 exhibited a strong correlation with the choice of the melt-annealing temperature (T_f) when T_f was less than about 160 °C, while it became independent of T_f when T_f was greater than about 160 °C. On the other hand, the half-time of crystallization of s-PP#8/$CaCO_3$ compounds did not vary much with the T_f. Generally, the observed half-time of crystallization decreased with increasing $CaCO_3$ content and increased with increasing $CaCO_3$ particle size. Finally, coating the surface of $CaCO_3$ particles with either stearic acid or paraffin reduced the ability of the particles to effectively nucleate s-PP#8. © 2006 Wiley Periodicals, Inc. J Appl Polym Sci 100: 4515–4525, 2006

Key words: syndiotactic polypropylene; calcium carbonate; composite; rheology; crystallization; melt-annealing

INTRODUCTION

Syndiotactic polypropylene (s-PP) of high regio- and stereo-regularities was successfully synthesized by Ewen et al.[1] using a metallocene catalytic system, instead of the traditional Ziegler–Natta catalytic system.[2] This has led to renewed interests in this polymer.[3–8] Despite some of its interesting properties, such as high ductility and high optical transparency, the syndiotactic form of PP (i.e., s-PP) has enjoyed less commercial utilization than its isotactic counterpart (i-PP).[9]

Among a number of drawbacks, the slow crystallization rate of s-PP is an important factor limiting the commercial utilization of this polymer.[10] Studies related to the crystallization process of semicrystalline polymers are of great importance in polymer processing, because the resulting physical properties of the products are strongly related to the extent of crystallization and the morphology formed. Both quiescent isothermal and nonisothermal melt-crystallization studies revealed that s-PP is a slowly crystallizing polymer.[10,11] The addition of nucleating agents may help enhance the crystallization rates by providing more sites for nucleation and therefore reducing the cycle time.

Nucleating agents can be either inorganic or organic substances. Some examples of inorganic nucleating agents are talcum, mica, barium sulfate ($BaSO_4$), and calcium carbonate ($CaCO_3$), and some examples of organic ones are sorbitols and their derivatives. Typically, $CaCO_3$ is added to i-PP to reduce the cost of the final product, to improve mechanical properties (e.g., modulus and heat stability), and to enhance the crystallization rate. Available reports on filled systems of s-PP have been concerned with their mechanical and thermal properties, including the phase behavior of s-PP filled with glass beads and talcum,[12–14] effects of $CaCO_3$ of varying size and surface modification on thermal and mechanical properties of s-PP/$CaCO_3$ compounds,[15] and effects of various organic and inorganic nucleating agents on crystallization and mechanical properties of nucleated s-PP systems.[16,17]

Correspondence to: P. Supaphol (pitt.s@chula.ac.th).
Contract grant sponsors: The Petroleum and Petrochemical Technology Consortium, The Petroleum and Petrochemical College, Chulalongkorn University

TABLE I
Characteristics of s-PP Resins Investigated

Polymer	M_n	M_w	M_z	M_w/Mz	Racemic pentads (%rrrr)	Racemic triads (%rr)	Racemic dyads (%r)	Ethylene content (% by wt)
s-PP#4	81,300	171,000	294,000	2.10	74.6	84.4	89.2	0.3
s-PP#5	47,000	165,000	406,000	3.51	75.3	85.1	90.0	0.2
s-PP#8	40,000	153,000	–	3.83	73.7	86.1	89.7	0.5

Studies related to processing of polymers cannot be complete without proper knowledge about their rheological characteristics. Studies related to rheological properties of s-PP are quite limited. In two related studies, Eckstein et al.[18,19] studied oscillatory shear behavior of various s-PP samples in comparison with both i-PP and atactic polypropylene (a-PP) samples. The only available report on steady state shear behavior of neat and $CaCO_3$-filled s-PP was by Supaphol et al.,[15] who showed that, for a given shear rate, the steady-state shear viscosity increased with increasing $CaCO_3$ loading.

In the present contribution, steady-state and oscillatory shear behavior of three different s-PP resins were investigated. The effects of $CaCO_3$ of varying particle size (1.9, 2.8, and 10.5 μm), content (0–40 wt %), and type of surface modification (uncoated, stearic acid-coated, and paraffin-coated) on steady-state and oscillatory shear behavior of $CaCO_3$-filled s-PP compounds were examined. The effects of melt-annealing and crystallization temperatures on isothermal crystallization behavior of neat s-PP and s-PP filled with $CaCO_3$ of varying particle size, content, and type of surface modification were also studied.

EXPERIMENTAL

Materials

Three commercial grades of syndiotactic polypropylene (s-PP) were supplied in the pellet form by Atofina Petrochemicals, Inc. (Houston, TX). Molecular characterization of these resins was carried out by Dr. Roger A. Phillips, formerly with Basell USA, Inc. (Elkton, Maryland). The results are summarized in Table I. Five commercial grades of calcium carbonate ($CaCO_3$) were supplied by Calcium Products Co., Ltd. (Thailand). Some important characteristics of these $CaCO_3$ grades (all having the density of about 2.7 g cm^{-3}) are summarized in Table II. Characterization of all of the $CaCO_3$ grades by X-ray diffraction (Cu Kα radiation, λ = 1.54 Å, Rigaku Rint2000 diffractometer) revealed that most of the as-received grades exhibited strong reflection peaks at scattering angles (2θ) of 29.0°, 39.4°, and 43.2°, corresponding to the characteristic peaks of calcite (JCPDS card no. 5–586), with an exception to the 10.5 μm-uncoated $CaCO_3$ grade (CALOFIL 50), which exhibited strong reflection peaks, in addition to those of calcite, at 2θ of 30.9°, 41.1°, and 51.0°, corresponding to those of calcium magnesium carbonate or dolomite ($CaMg(CO_3)_2$) (JCPDS card no. 36–426).

Sample preparation

$CaCO_3$ of varying particle size and type of surface treatment (i.e., uncoated, stearic acid-coated, or paraffin-coated) was first dried in an oven at 80°C for 14 h and then premixed with s-PP#8 resin in a tumble mixer for 10 min in various compositional ratios, ranging from 0 to 40 wt % (about 0–18 vol %). The premixed compounds were then melt-mixed in a Collin ZK25 self-wiping, corotating twin-screw extruder operating at a screw speed of 50 rpm and the die temperature of 190°C. The extrudate was cooled in water and then pelletized using a Planetrol 075D2 pelletizer. A Wabash V50H compression press was used to prepare films and sheets from all of the neat s-PP resins and the as-prepared s-PP#8/$CaCO_3$ compounds for subsequent tests. The mold was first preheated in the compression press at 190°C for 5 min and then compressed with a 15 ton-force for another 5 min, after which it was cooled to 40°C.

Rheological measurement

The steady-shear measurement for all of the neat s-PP resins and the as-prepared s-PP#8/$CaCO_3$ compounds was carried out using two types of rheometers. An ARES Rheometric Scientific rheometer with a parallel-plate geometry (a 8 mm diameter and a 0.2 mm gap width) was used to study the steady-state shear be-

TABLE II
Characteristics of $CaCO_3$ Investigated

Trade name	Specific surface area (cm^2 g^{-1})	Average particle size (μm)	Surface modification
CALOFIL 400	13,000	1.9	Uncoated
CALOFIL 100	10,500	2.8	Uncoated
CALOFIL 50	5000	10.5	Uncoated
HICOAT 410	13,000	1.9	Stearic acid-coated
HICOAT P400	13,000	1.9	Paraffin-coated

havior of these samples at "low" shear rates (from about 0.25 to 25 rad s^{-1}). The measurement was performed on the steady-rate sweep test. An Instron 3213 capillary rheometer was used to study the steady-state shear behavior of these samples at "high" shear rates (from about 50 to 3000 s^{-1}). The capillary was a tapered type having a 45° entrance angle. The barrel diameter was 9.525 mm and the number 1860 capillary die (1.25 mm diameter, 50.19 mm length, and a L/D ratio of 40.15) was used. The dynamic viscoelastic properties of these samples were carried out on the ARES Rheometric Scientific rheometer with the aforementioned parallel-plate geometry. The dynamic-strain sweep test was used to obtain the linear viscoelastic regime at a frequency of 1 rad s^{-1}. After that the dynamic frequency sweep test was used to measure the storage G' and the loss modulus G'', covering a frequency range of 0.05–100 rad s^{-1}.

All of the measurements on neat s-PP resins were carried out over a temperature range of 180–220°C, with a master curve being constructed at a reference temperature of 200°C. In the case of s-PP#8/$CaCO_3$ compounds however, the measurements were carried out at a fixed temperature of 200°C.

Isothermal crystallization measurement

A PerkinElmer Series 7 differential scanning calorimeter (DSC) was used to investigate the isothermal crystallization characteristics of neat s-PP#8 and s-PP#8/$CaCO_3$ samples. Calibration for the temperature scale of the DSC furnaces was carried out using a pure indium standard on every other run to ensure accuracy of the data obtained. Each sample holder was loaded with a disc-shape sample cut from the as-prepared films. Each sample weighed around 5.0 ± 0.8 mg and was used only once. All the experimental runs were carried out under a nitrogen atmosphere.

In studies related to isothermal crystallization behavior of s-PP#8 filled with $CaCO_3$ particles of varying size (1.9, 2.8, or 10.5 μm), content (0, 20, or 40 wt %), and type of surface modification (uncoated, stearic acid-coated, or paraffin-coated), the effects of different choices of the melt-annealing temperature (T_f) used to melt and choices of the crystallization temperature (T_c) used to crystallize the samples on subsequent crystallization characteristics of these compounds are of our prime concern. Studies about the effect of different choices of the T_f on the primary crystallization behavior of s-PP should reveal a great deal about the primary nucleation behavior of s-PP in response to the variation in size, content, and type of surface modification of $CaCO_3$ particles. On the other hand, studies about the effect of different choices of the T_c on the primary crystallization behavior of s-PP should reveal a great deal about the overall crystallization behavior of s-PP in response to the variation in size, content, and type of surface modification of $CaCO_3$ particles.

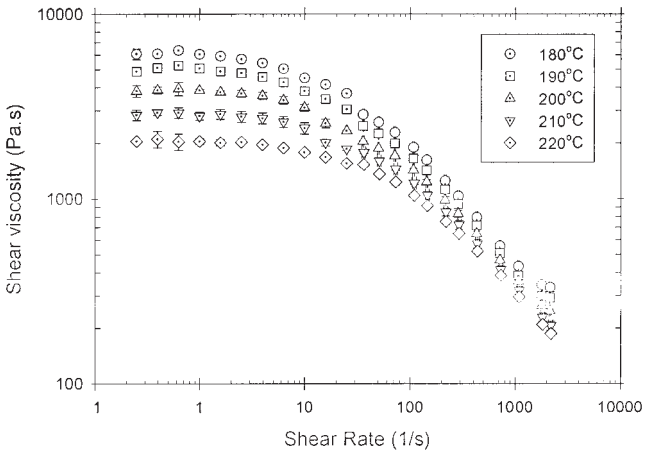

Figure 1 Steady-state shear viscosity as a function of shear rate for s-PP#4 at various temperatures.

To study the effect of melt-annealing temperature (T_f) on isothermal crystallization characteristics of neat s-PP#8 and s-PP#8/$CaCO_3$ samples, each experimental run was started with heating each sample from room temperature at 80°C min^{-1} to a T_f, ranging from about 127 to 230°C. After a fixed melt-annealing period (t_h) of 5 min, each sample was rapidly cooled at a rate of about 200°C min^{-1} from the T_f to a fixed crystallization temperature (T_c) of 90°C, where it was held until the primary crystallization process was considered complete. To study the effect of T_c on isothermal crystallization characteristics of neat s-PP#8 and s-PP#8/$CaCO_3$ samples, each experimental run was started with heating each sample from room temperature to a fixed T_f value of 190°C for a fixed t_h value of 5 min. Subsequently, each sample was rapidly cooled at a rate of about 200°C min^{-1} from 190°C to completely crystallize at three different T_c values of 87.5, 90, and 92.5°C.

RESULTS AND DISCUSSION

Rheological properties of neat s-PP resins

Figure 1 shows steady shear viscosity of s-PP#4 as a function of shear rate at five different temperatures ranging from 180 to 220°C. Apparently, within the low shear rate region, the viscosity at a given temperature did not seem to vary with the shear rate and it approached a constant value at very low shear rates, i.e., the zero shear-rate viscosity (η_0). In the higher shear rate region however, the viscosity decreased monotonically with increasing shear rate, an indication of a shear-thinning behavior of this material. As expected, at a given shear rate, the steady shear viscosity was a decreasing function of the temperature. Generally, s-

PP#5 and s-PP#8 resins exhibited a similar behavior to what was observed for s-PP#4.

The temperature-dependent melt viscosity-shear rate data for all of the s-PP resins investigated can be superimposed into a master curve at a reference temperature (T_0) by dividing the shear viscosity values with a shift factor (a_T) and simultaneously multiplying the shear rate values with the same a_T. After plotting the shifted shear viscosity versus the shifted shear rate, the master curve is obtained. The shift factor a_T is simply a ratio between the viscosity values at a given temperature to those at a chosen T_0, i.e., $a_T = \eta(T)/\eta(T_0)$. In the present work, T_0 was chosen to be 200°C. Figure 2 shows the obtained master curves for all of the neat s-PP resins investigated, and corresponding a_T values are summarized in Table III. According to Figure 2, it is obvious that the time–temperature superposition for s-PP#4 and s-PP#5 resins was of good quality, while that for s-PP#8 resin was relatively poor. This could be a result of the very wide molecular weight distribution of s-PP#8 resin in comparison with the other two resins.

Normally, the temperature dependence of a_T can be expressed in terms of either an Arrhenius equation[18,19]

$$\log a_T = \frac{E_a}{2.303R}\left(\frac{1}{T} - \frac{1}{T_0}\right) \quad (1)$$

where R is the universal gas constant (R = 8.314 J mol^{-1} K^{-1}) and E_a is the activation energy of flow, or the Williams–Landel–Ferry (WLF) equation:[18,19]

$$\log a_T = \frac{-c_1(T - T_0)}{c_2 + (T - T_0)} \quad (2)$$

where c_1 and c_2 are the WLF parameters. Though the WLF equation is normally restricted to a limited temperature range around T_g (i.e., $T_g - 50 \leq T \leq T_g + 100$), its use in the present contribution was to compare with the literature.[18,19] The validity of both the Arrhenius and the WLF equations in describing the obtained data was checked by fitting the a_T values of each s-PP resin to both equations. All of the parameters characteristic to both equations are summarized in Table IV.

For all of the s-PP resins investigated, the a_T varied from about 0.5 to 2.0 over a range of the test temperatures of 40°C. These factors are comparable to those reported earlier by Eckstein et al.[18] of about 0.3–1.5, which indicated a small temperature dependence of this polymer with regards to its rheological behavior in comparison with other linear polymers such as polystyrene (PS) or poly(methyl methacrylate) (PMMA). Both the Arrhenius and the WLF equations provided good fits to the experimental data. The c_1 ranged between about 3.8 and 4.9, while

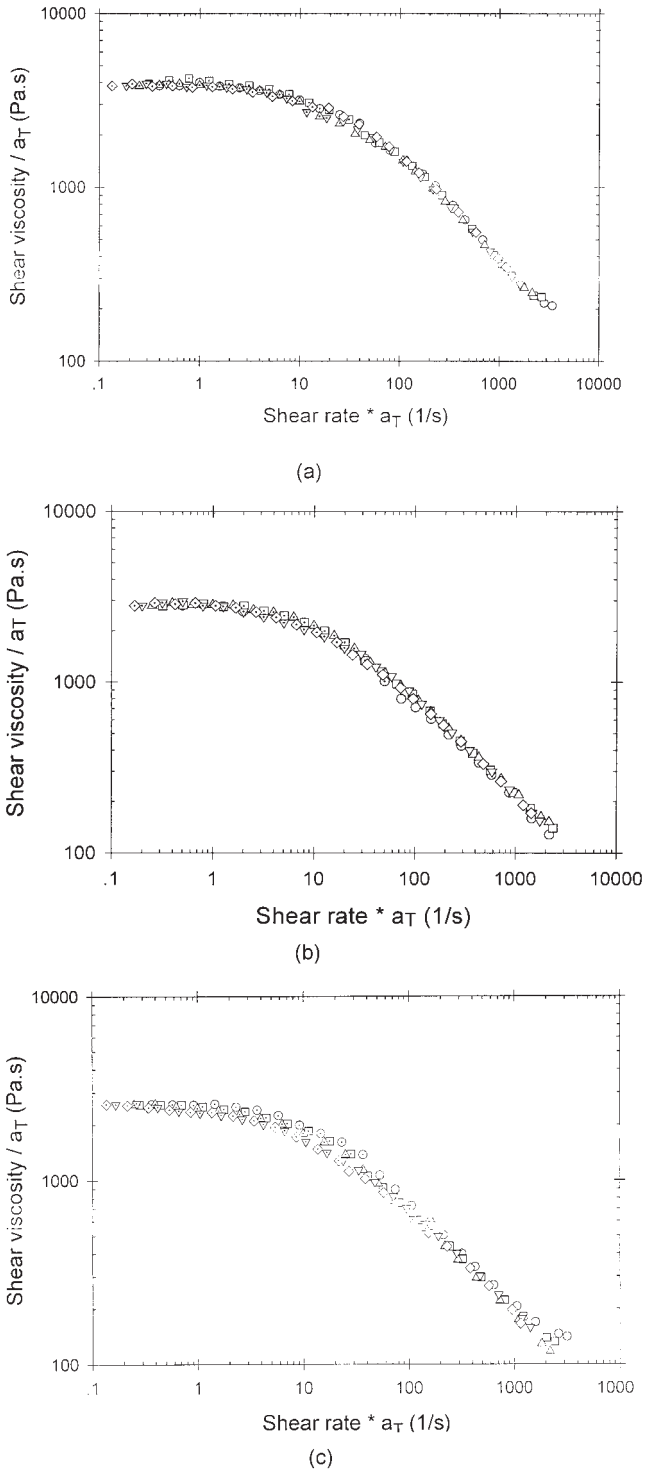

Figure 2 Master curves of reduced shear viscosity as a function of reduced shear rate for (a) s-PP#4, (b) s-PP#5, and (c) s-PP#8 at the reference temperature of 200°C.

the c_2 for all of the s-PP resins was identical (400.1 K). Eckstein et al.[18,19] reported the c_1 to be about 3.4–9.2, while the c_2 to be about 241–473 K. The E_a signifying the activation energy of flow for all of the s-PP resins investigated ranged between 47 and 50

TABLE III
Shift factor of s-PP Resins Investigated

Temperature (°C)	Shift factor, a_T		
	s-PP#4	s-PP#5	s-PP#8
180	1.587	2.003	1.817
190	1.244	1.276	1.397
200	1.000	1.000	1.000
210	0.743	0.799	0.805
220	0.535	0.672	0.678

kJ mol^{-1}. Eckstein et al. reported the E_a of various s-PP resins to be about 49–74 kJ mol^{-1},[18,19] while that of various i-PP resins ranged between 38 and 43 kJ mol[18,19] and that of an atactic polypropylene (a-PP) resin was 39 kJ mol^{-1}.[19] The observed greater E_a values of s-PP resins in comparison with those of i-PP suggested the greater resistance to flow, likely a result of the observed greater molecular entanglement density.[20]

Figure 3 shows both the storage (G') and loss moduli (G'') of neat s-PP#4 resin at various temperatures ranging between 180 and 220°C over a frequency range of about 0.07 to 100 rad s^{-1}. Obviously, for a given temperature, both G' and G'' increased with increasing frequency and, for a given frequency, both G' and G'' decreased with increasing temperature, or vice versa. In a similar manner with the steady shear experiments, isotherms of G' (ω,T) and G'' (ω,T) can be superimposed by a horizontal shift along the frequency axis (ω) to a reference temperature (T_0 = 200°C), using the a_T values summarized in Table III, from which the resulting master curves [G' (ωa_T,T_0) and G'' (ωa_T,T_0)] are illustrated in Figure 4. Apparently, for all of the s-PP resins investigated, G'' was proportional to ω in the terminal zone, in which the slope was close to 1 in a double logarithmic plot, while G' showed a slight deviation from the slope of 2, which could mean that the terminal zone was not finally reached. Interestingly, the results were essentially similar to those reported by Eckstein et al.[18]

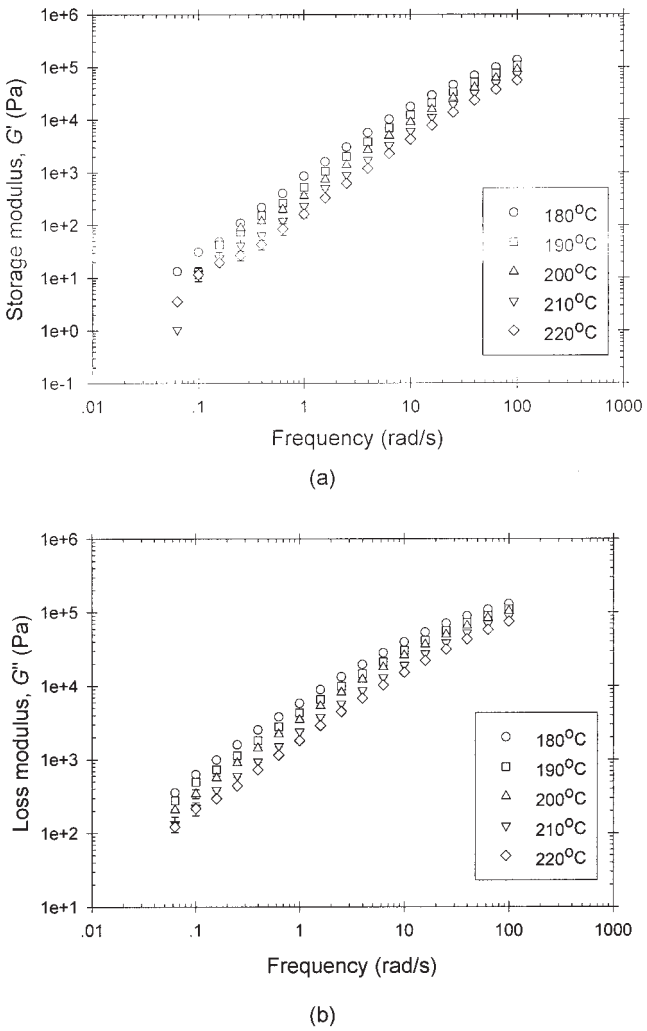

Figure 3 (a) Storage and (b) loss moduli of s-PP#4 at five different temperatures.

Rheological properties of s-PP#8/$CaCO_3$ compounds

The steady-state shear behavior of s-PP#8/$CaCO_3$ compounds was measured over a shear rate range of 0.25–3000 s^{-1} at 200°C, using both parallel-plate (to cover a shear rate range of 0.25–25 s^{-1}) and capillary rheometers (to cover a shear rate range of 50–3000 s^{-1}). Dependence of the steady-state shear viscosity of s-PP#8/$CaCO_3$ compounds on content, particle size, and type of surface modification of $CaCO_3$ particles was investigated.

The steady-state shear viscosity of neat s-PP#8 and 1.9 μm-uncoated $CaCO_3$-filled s-PP#8 samples of various filler contents as a function of shear rate is shown in Figure 5(a). Apparently, neat s-PP#8 and 1.9 μm-uncoated $CaCO_3$-filled s-PP#8 samples of "low" filler loadings (about 5–20 wt %) exhibited the typical shear thinning behavior, with a plateau region being observed at low shear rates (< about 1 s^{-1}) and a shear thinning region at higher shear rates (> about 1 s^{-1}). At higher filler loadings (> 20 wt %) however, the compounds exhibited shear thinning behavior as well, but without the presence of a plateau region at low shear rates, and the viscosity values were always non-

TABLE IV
WLF Parameters and Activation Energy of Flow of s-PP Resins Investigated

Polymer	c_1	c_2 (K)	c_1c_2 (K)	E_a (kJ mol^{-1})
s-PP#4	3.8	400.1	1525.3	49.9
s-PP#5	4.1	400.1	1652.2	49.5
s-PP#8	4.9	400.1	1972.0	47.0

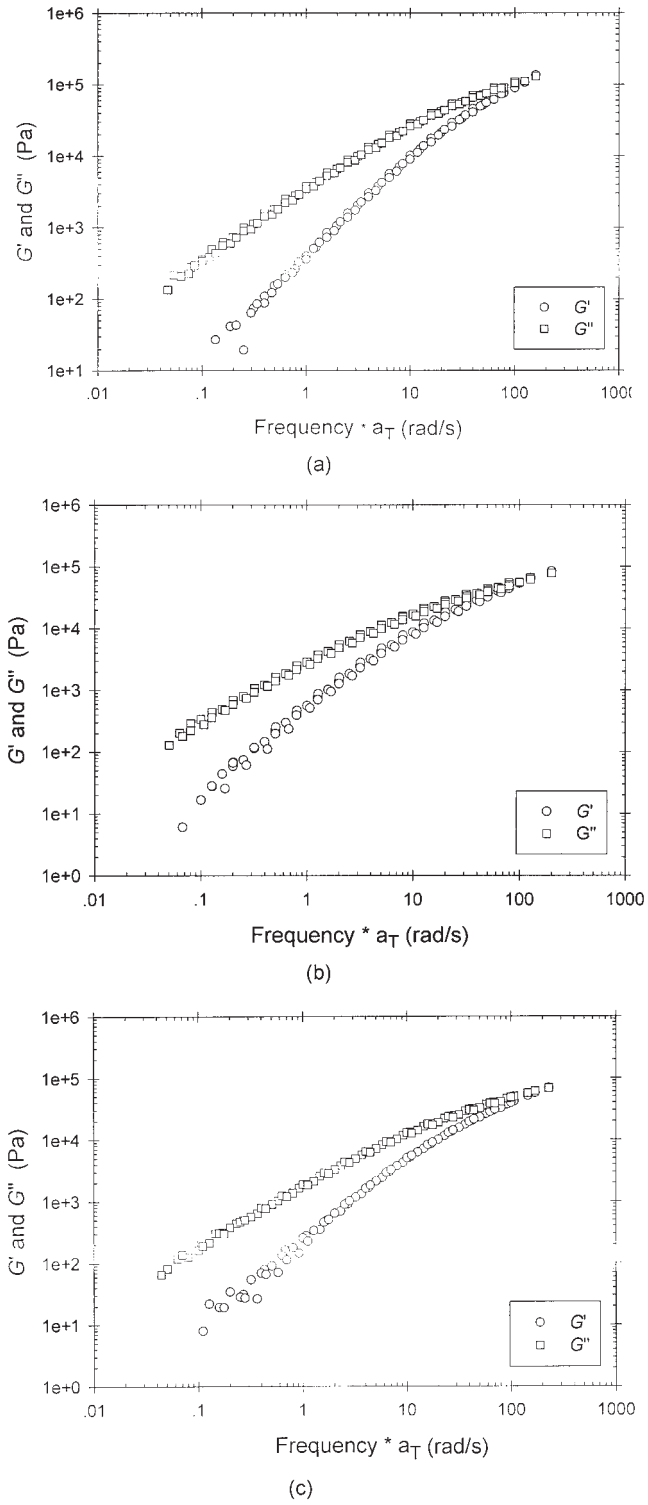

Figure 4 Master curves of storage and loss moduli as a function of reduced frequency for (a) s-PP#4, (b) s-PP#5, and (c) s-PP#8 at the reference temperature of 200°C.

Newtonian and became increasingly nonlinear and unbounded with decreasing shear rate. Such an unbounded shear viscosity represents yielding as predicted by most viscoelastic models, where the apparent viscosity tends to infinity at vanishing shear rates, a direct result of the presence of yield stress below which there is no flow.[21,22] The other compounds filled with $CaCO_3$ particles of larger sizes (2.8 and 10.5 μm) also exhibited a similar behavior to what has been described earlier.

Figure 5(b) compares the values of the shear viscosity at the shear rate of about 0.25 s^{-1} (hereafter, 0.25 s^{-1}-shear viscosity) of neat s-PP#8 and s-PP#8 samples filled with $CaCO_3$ particles of varying particle size as a function of $CaCO_3$ content. Apparently, the 0.25 s^{-1}-shear viscosity values increased monotonically with increasing filler loading. The enhancement in the shear viscosity due to the presence of noninteractive rigid particles in dilute suspensions was proposed long ago by Einstein,[23,24] who pointed out that the enhancement in the shear viscosity was a result of increased energy dissipation attributable to the pres-

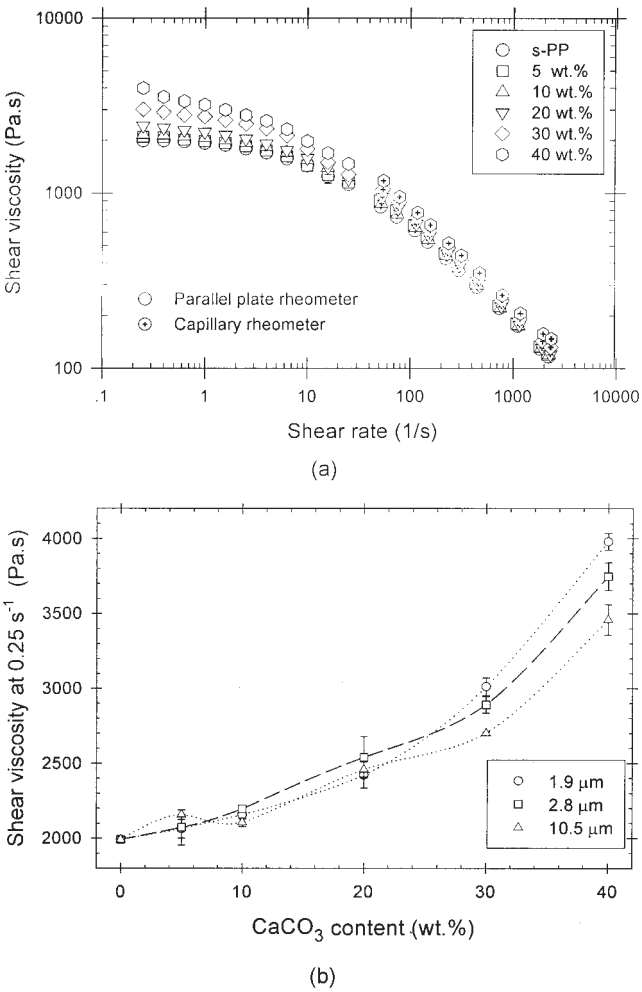

Figure 5 (a) Steady-state shear viscosity as a function of shear rate for neat s-PP#8 and s-PP#8 filled with 1.9 μm uncoated $CaCO_3$ particles of varying content at 200°C and (b) shear viscosity at 0.25 s^{-1} as a function of $CaCO_3$ content for neat s-PP#8 and s-PP#8 filled with uncoated $CaCO_3$ of varying particle size.

ence of the particles. In more concentrated suspensions, stronger interactions between filler particles give rise to a much larger energy dissipation, resulting in a much increase in the shear viscosity.[25] This is exactly the reason for the observed increase in the 0.25 s^{-1}-shear viscosity values at high filler loadings observed for these s-PP#8/$CaCO_3$ compounds. Additionally, among s-PP#8 samples loaded with uncoated $CaCO_3$ particles at high filler loadings (about >20 wt %), 1.9 μm-uncoated $CaCO_3$-filled s-PP#8 samples exhibited the highest 0.25 s^{-1}-shear viscosity value. It is a known fact that the smaller the filler particles, the larger the surface area, giving rise to a greater possibility for the formation of interparticular structure. As a result of the strong interparticular interactions, the enhancement in the shear viscosity for the sample filled with these fine $CaCO_3$ particles was apparent.

The steady-state shear viscosity of neat s-PP#8 and 1.9 μm-stearic acid-coated $CaCO_3$-filled s-PP#8 samples of varying $CaCO_3$ content as a function of shear rate is shown in Figure 6(a). The 1.9 μm-paraffin-coated $CaCO_3$-filled s-PP#8 samples, though not shown, also exhibited a similar behavior. Obviously, the compounds filled with coated $CaCO_3$ particles exhibited a similar behavior to those filled with uncoated ones [see Fig. 5(a)]. Interestingly at high shear rates, the steady-state shear viscosity of s-PP#8 filled with coated $CaCO_3$ particles did not seem to vary much with variation in the filler content, suggesting no interparticular structure being formed for these coated particles.[22] For better representation of the results, comparison of the 0.25 s^{-1}-shear viscosity values obtained for compounds filled with $CaCO_3$ particles of varying filler loading and type of surface modifications is illustrated in Figure 6(b). The 0.25 s^{-1}-shear viscosity values of s-PP#8 filled with stearic acid-coated and paraffin-coated $CaCO_3$ particles were slightly lower than those of s-PP#8 filled with uncoated $CaCO_3$ particles, especially at high filler loadings (about >10 wt %), confirming that interparticular interactions of $CaCO_3$ particles was reduced as a result of the surface modification.

The oscillatory shear behavior of s-PP#8/$CaCO_3$ compounds was measured over a frequency sweep range of 0.1–100 rad s^{-1} at 200°C. All tests were carried out at a fixed strain amplitude of 20%, corresponding to the linear viscoelastic region. Dependence of the storage and the loss moduli of s-PP#8 filled with 1.9 μm $CaCO_3$ particles of varying content and type of surface modification was investigated.

Figure 7 shows both G' and G'' of neat s-PP#8 and s-PP#8 filled with 1.9 μm uncoated $CaCO_3$ particles in various contents. Though not shown, other compounds of s-PP#8 filled with 1.9 μm surface-coated $CaCO_3$ particles also showed a similar behavior. Storage modulus represents the elastic response of a material, which relates to the potential energy stored by

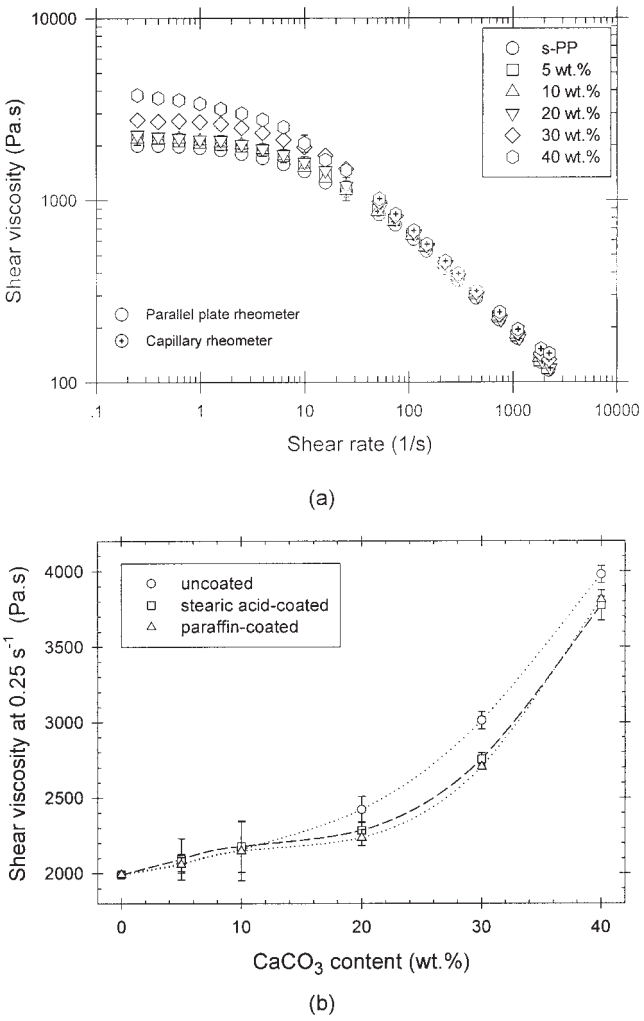

Figure 6 (a) Steady-state shear viscosity as a function of shear rate for neat s-PP#8 and s-PP#8 filled with 1.9 μm stearic acid-coated $CaCO_3$ particles of varying content at 200°C and (b) shear viscosity at 0.25 s^{-1} as a function of $CaCO_3$ content for neat s-PP#8 and s-PP#8 filled with 1.9 μm $CaCO_3$ particles of varying type of surface treatment.

the material during deformation. The value of the storage modulus thus represents the stiffness of the material. On the contrary, loss modulus represents the viscous response of the material. The value of the loss modulus thus signifies the dissipation of energy in the form of heat during deformation. According to Figure 7, both the elastic and the viscous behavior of filled s-PP#8 systems exhibited the variation in the property values with the frequency in a similar manner. For s-PP#8 filled with uncoated $CaCO_3$ particles, the increase in both G' and G'' values with increasing $CaCO_3$ content at a low frequency region was much larger than that at a higher frequency region. At low frequencies, interparticular interactions of $CaCO_3$ particles could be a factor contributing to the much increase in both values; however, interparticular interactions became less dominant at higher frequencies.[25] When the

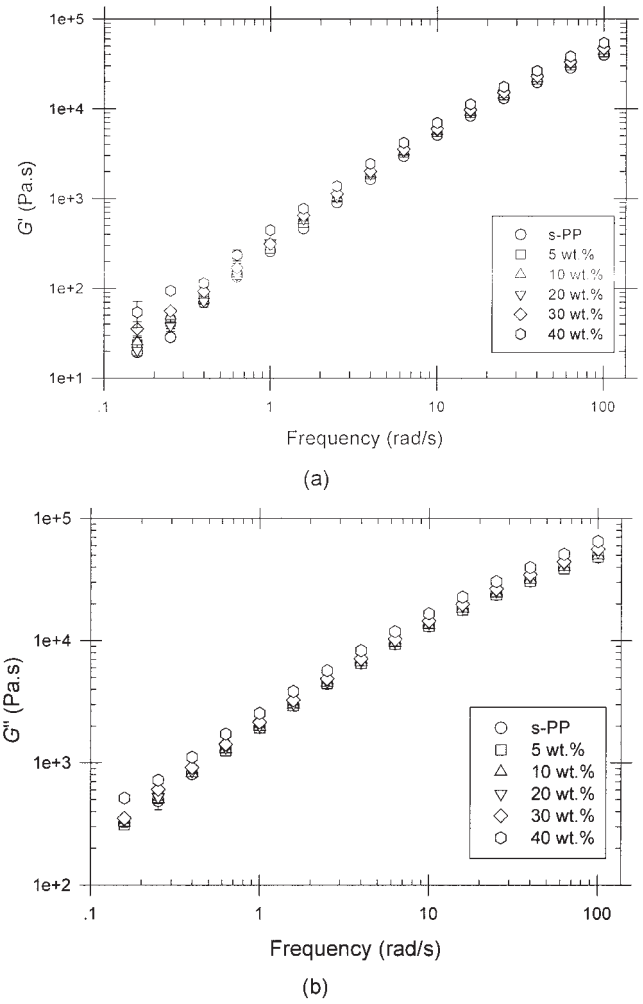

Figure 7 (a) Storage and (b) loss moduli as a function of frequency for neat s-PP#8 and s-PP#8 filled with 1.9 μm uncoated $CaCO_3$ particles of varying content at 200°C.

surface of $CaCO_3$ particles was coated with either stearic acid or paraffin, the increase in both G' and G'' values at a low frequency region (results not shown) was much less pronounced. The absence of the interparticular interactions could be a reason for such observation.

Isothermal crystallization behavior of neat sPP#8 and s-PP#8/$CaCO_3$ compounds

In DSC, studies related to the crystallization process can be carried out by following the crystallization exotherms, based on the notion that the evolution of crystallinity is linearly proportional to the evolution of heat throughout the course of crystallization. As a result, the relative crystallinity as a function of time [$\theta(t)$] can be approximated according to the following equation

$$\theta(t) = \frac{\int_0^t \left(\frac{dH_c}{dt}\right) dt}{\int_0^\infty \left(\frac{dH_c}{dt}\right) dt} \in [0,1] \quad (3)$$

where t and ∞ are the elapsed time during the course of crystallization and at the end of crystallization process, respectively, and dH_c is the enthalpy of crystallization released during an infinitesimal time interval dt.

The simplest representation of the overall crystallization rate of semicrystalline polymers is through the use of the half-time of crystallization ($t_{0.5}$), defined as the elapsed time interval from the onset of crystallization to the point where the primary crystallization process is half-completed. With such a definition, a $t_{0.5}$ value can be obtained directly from an experimental $\theta(t)$ function. The qualitative relationship of the $t_{0.5}$ value and the overall crystallization kinetics is straightforward in the sense that the larger the $t_{0.5}$ value, the slower the crystallization rate (or vice versa).

Effect of melt-annealing temperature

Figure 8 illustrates the effect of T_f on the half-time of crystallization ($t_{0.5}$) of neat s-PP#8 and s-PP#8 filled with uncoated 1.9 μm $CaCO_3$ particles of varying content (20 or 40 wt %). The T_c investigated was fixed

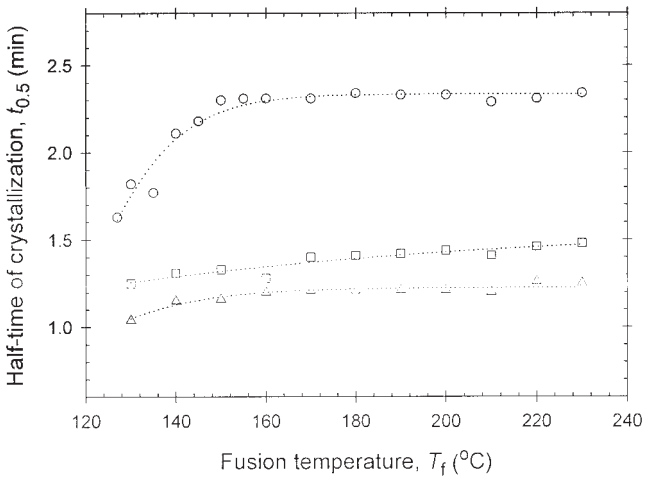

Figure 8 Half-time of crystallization as a function of melt-annealing temperature for (○) neat s-PP#8 and s-PP#8 filled with (□) 20 and (△) 40 wt % 1.9 μm uncoated $CaCO_3$ particles.

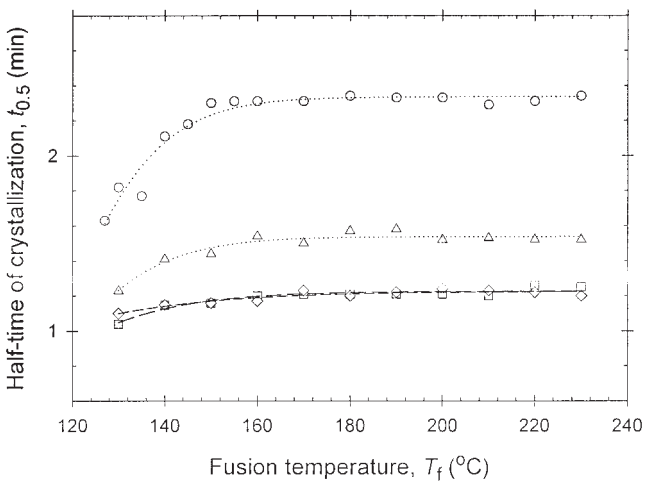

Figure 9 Half-time of crystallization as a function of melt-annealing temperature for (○) neat s-PP#8 and s-PP#8 filled with 40 wt % (□) 1.9, (△) 2.8, and (◇) 10.5 μm uncoated $CaCO_3$ particles.

at 90°C. The observed $t_{0.5}$ value of pure s-PP#8 seems to have a strong correlation with the T_f, especially in the range where T_f was less than about 160°C, while it became independent of the T_f when $T_f > \sim 160$°C. The results suggested that prolonged melting of s-PP#8 at a T_f greater than about 160°C for 5 min was sufficient to erase all of the crystalline residues, rendering any measurement on subsequent crystallization behavior to be free from the influence of the self-nucleation effect.[26] Interestingly, despite the different nature of the s-PP resin investigated here in comparison with other s-PP resins investigated in a previous report, similar results were obtained in that the critical T_f that was needed for these s-PP resins to attain the complete molten state after 5 min of melt-annealing period (t_h) was essentially identical (160°C).[26] Moreover, the $t_{0.5}$ values for s-PP#8 filled with both 20 and 40 wt % 1.9 μm uncoated $CaCO_3$ particles did not vary much with the T_f, possibly a result of the enhanced nucleation rates attributable to the presence of the $CaCO_3$ particles[15] and that the $t_{0.5}$ values for s-PP#8 filled with 20 wt % $CaCO_3$ particles were systematically greater than those for s-PP#8 filled with 40 wt % $CaCO_3$ particles, suggested that an increase in the filler content enhanced the crystallization rates of the resulting compounds.

Figure 9 shows dependence of the $t_{0.5}$ on the choice of the T_f for neat s-PP#8 and s-PP#8 filled with 40 wt % $CaCO_3$ particles of varying size (1.9, 2.8, or 10.5 μm). In a similar manner to the filled s-PP#8 systems shown previously, the $t_{0.5}$ values for all of the s-PP#8 samples filled with $CaCO_3$ of varying particle size did not vary much with the choice of the T_f. For a given T_f investigated, the $t_{0.5}$ value of neat s-PP#8 was the greatest, followed by those of s-PP#8 filled with 40 wt % 2.8 and 1.9 μm $CaCO_3$ particles, respectively, suggesting that the ability for 1.9 μm $CaCO_3$ particles to nucleate s-PP#8 was better than that of 2.8 μm $CaCO_3$ particles. Clearly, the greater surface area of $CaCO_3$ particles of smaller size gave rise to the observed increased nucleation efficiency.[15] Surprisingly, the $t_{0.5}$ value of 10.5 μm-uncoated $CaCO_3$-filled s-PP#8 (instead of being in between those of 2.8 μm-uncoated $CaCO_3$-filled and neat s-PP#8) was almost identical to that of 1.9 μm-uncoated $CaCO_3$-filled s-PP#8. As previously reported,[15] the presence of dolomite or $CaMg(CO_3)_2$ was postulated to be the reason for the observed increase in the nucleation ability of 10.5 μm $CaCO_3$ particles.

Figure 10 illustrates the variation of the $t_{0.5}$ on the choice of the T_f for neat s-PP#8 and s-PP#8 filled with 40 wt % 1.9 μm $CaCO_3$ particles of different surface modificiations (uncoated, stearic acid-coated, and paraffin-coated). Apparently, the $t_{0.5}$ values for all of the s-PP#8 samples filled with either uncoated or coated $CaCO_3$ particles did not vary much with the choice of the T_f. For a given T_f investigated, the $t_{0.5}$ value of neat s-PP#8 was the greatest, followed by those of s-PP#8 filled with either stearic acid- or paraffin-coated and uncoated $CaCO_3$ particles, respectively, suggesting that 1.9 μm $CaCO_3$ particles were less efficient in nucleating s-PP#8 when their surface was coated with either stearic acid or paraffin.[15]

Effect of crystallization temperature

Table V summarizes the observed $t_{0.5}$ values for neat and filled s-PP#8 samples to illustrate the effects of content, size, and surface modification of $CaCO_3$ particles on the overall crystallization kinetics of s-PP#8/$CaCO_3$ compounds. The samples were crystallized at three different T_c values (87.5, 90, and 92.5°C) after

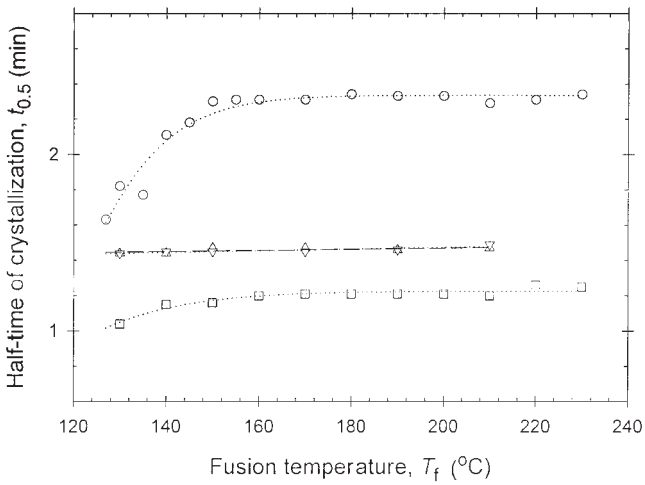

Figure 10 Half-time of crystallization as a function of melt-annealing temperature for (○) neat s-PP#8 and s-PP#8 filled with 40 wt % 1.9 μm (□) uncoated, (△) stearic acid-coated, and (▽) paraffin-coated $CaCO_3$ particles.

TABLE V
Effect of Crystallization Temperature on Isothermal Crystallization Characteristics of Neat s-PP#8 and Various s-PP#8/$CaCO_3$ Compounds

Materials	Half-time of crystallization $t_{0.5}$ (min)		
	T_c = 87.5°C	T_c = 90°C	T_c = 92.5°C
Neat s-PP#8	1.82	2.33	4.05
20 wt % 1.9 μm uncoated $CaCO_3$-filled s-PP#8	0.95	1.42	1.85
40 wt % 1.9 μm uncoated $CaCO_3$-filled s-PP#8	0.88	1.21	1.56
40 wt % 2.8 μm uncoated $CaCO_3$-filled s-PP#8	1.23	1.58	1.84
40 wt % 10.5 μm uncoated $CaCO_3$-filled s-PP#8	0.95	1.22	1.65
40 wt % 1.9 μm uncoated $CaCO_3$-filled s-PP#8	1.14	1.46	1.85
40 wt % 1.9 μm stearic acid-coated $CaCO_3$-filled s-PP#8	1.06	1.44	1.92

they were completely melt at 190°C for 5 min. For a given sample type, increased T_c resulted in an increase in the $t_{0.5}$ value, suggesting decreased crystallization rate with increasing T_c, as normally would for the crystallization in the nucleation-controlled region.[27] For a given T_c, the observed $t_{0.5}$ was found to decrease with increasing $CaCO_3$ content and increase with increasing $CaCO_3$ particle size (except for that of s-PP#8 filled with 10.5 μm $CaCO_3$ particles). Evidently, the presence of both stearic acid and paraffin on the surface of $CaCO_3$ particles resulted in the resulting composites having the $t_{0.5}$ values greater than that of the composites filled with the uncoated ones.

CONCLUSIONS

Steady-state and oscillatory shear behavior of three neat syndiotactic polypropylene (s-PP) resins and a s-PP resin (s-PP#8) filled with $CaCO_3$ particles of varying content, size, and type of surface modification were investigated. Over the temperature range investigated (180 to 220°C), all of the neat s-PP resins investigated exhibited the expected shear-thinning behavior. Master curves of the steady-state shear viscosity of all three neat resins were constructed by both horizontal and vertical shifting of the experimental data at a reference temperature to 200°C. The shift factor (a_T) ranged between 0.5 and 2.0. Both the Arrhenius and the Williams–Landel–Ferry provided a good fit to the a_T values obtained. Both the storage and loss moduli, measured over a temperature range of 180–220°C, increased with decreasing temperature. Based on the a_T values obtained earlier, master curves of both the storage and loss moduli were successfully constructed.

The inclusion of $CaCO_3$ particles of varying content, size, and type of surface modification, to a large extent, affected both the steady-state and oscillatory shear behavior of s-PP/$CaCO_3$ compounds. The shear viscosity at the shear rate of 0.25 s^{-1} (i.e., 0.25 s^{-1}-shear viscosity) increased monotonically with increasing $CaCO_3$ content, with the samples loaded with 1.9 μm uncoated $CaCO_3$ particles exhibiting the greatest value, likely a result of the formation of interparticular structures of these small, rigid particles that had the largest surface area. The 0.25 s^{-1}-shear viscosity was however reduced when the surface of $CaCO_3$ particles was coated with either stearic acid or paraffin, possibly a result of the reduced interparticular interactions. The storage and loss moduli of s-PP/$CaCO_3$ compounds were both found to increase with increasing frequency, with the increase in both quantities with increasing $CaCO_3$ content at a low frequency region was more pronounced than that at a higher frequency region, possibly a result of the interparticular interactions of $CaCO_3$ particles.

The effects of melt-annealing and crystallization temperatures on isothermal crystallization behavior of s-PP#8 filled with $CaCO_3$ particles of varying content, size, and type of surface modification were also investigated. The half-time of crystallization of neat s-PP#8 exhibited a strong correlation with the choice of the melt-annealing temperature (T_f) when $T_f < \sim$160°C, while it became independent of T_f when $T_f > \sim$160°C. The results suggested that prolonged melting of s-PP#8 at a T_f greater than about 160°C for 5 min was sufficient for the polymer to attain the complete molten state. On the other hand, the half-time of crystallization of s-PP#8/$CaCO_3$ compounds did not vary much with the choice of T_f. For a given sample type, increased crystallization temperature (T_c) resulted in an increase in the half-time of crystallization. For a given T_c, the observed half-time of crystallization decreased with increasing $CaCO_3$ content and increased with increasing $CaCO_3$ particle size. Lastly, coating the surface of $CaCO_3$ particles with either stearic acid or paraffin reduced the ability for the particles to effectively nucleate s-PP#8.

The authors thank ATOFINA Petrochemicals, Inc. for supplying s-PP resins, Calcium Products Co., Ltd. for supplying various grades of $CaCO_3$, and Dr. Roger A. Phillips (formerly of Basell USA, Inc.) for carrying out molecular weight and syndiotacticity measurement of s-PP resins.

References

1. Ewen, J. A.; Johns, R. L.; Razavi, A.; Ferrara, J. D. J Am Chem Soc 1988, 110, 6255.
2. Natta, G.; Pasquon, I.; Zambelli, A. J Am Chem Soc 1962, 84, 1488.
3. Rodriguez-Arnold, J.; Bu, Z.; Cheng, S. Z. D. J Macromol Sci Rev Macromol Chem Phys 1995, C35, 117.
4. Schardl, J.; Sun, L.; Kimura, S.; Sugimoto, R. J Plast Film Sheeting 1996, 12, 157.
5. Sun, L.; Shamshoum, E.; DeKunder, G. SPE-ANTEC Proc 1996, 1965.
6. Gownder, M.; SPE-ANTEC Proc 1998, 1511.
7. Sura, R. K.; Desai, P.; Abhiraman, A. S.; SPE-ANTEC Proc 1999, 1764.
8. Guadagno, L.; Naddeo, C.; D'Aniello, C.; Di Maio, L.; Vittoria, V.; Acierno, D. Macromol Symp 2002, 180, 23.
9. Loos, J.; Bonner, M.; Petermann, J. Polymer 2000, 41, 351.
10. Supaphol, P.; Spruiell, J. E.; J Appl Polym Sci 2000, 75, 44.
11. Supaphol, P.; J Appl Polym Sci 2000, 78, 338.
12. Stricker, F.; Bruch, M.; Mülhaupt, R. Polymer 1997, 38, 5347.
13. Stricker, F.; Mülhaupt, R.; Polym Eng Sci 1998, 38, 1463.
14. Stricker, F.; Maier, R.-D.; Bruch, M.; Thomann, R.; Mülhaupt, R. Polymer 2077 1999, 40.
15. Supaphol, P.; Harnsiri, W.; Junkasem, J. J Appl Polym Sci 2004, 92, 201.
16. Supaphol, P.; Charoenphol, P.; Junkasem, J. Macromol Mater Eng 2004, 289, 818.
17. Charoenphol, P.; Supaphol, P. J Appl Polym Sci 2005, 95, 245.
18. Eckstein, A.; Friedrich, C.; Lobbrecht, A.; Spitz, R.; Mülhaupt, R. Acta Polymer 1997, 48, 41.
19. Eckstein, A.; Suhm, J.; Friedrich, C.; Maier, R.-D.; Sassmannshausen, J.; Bochmann, M.; Mülhaupt, R. Macromolecules 1998, 31, 1335.
20. Wheat, W. R. SPE-ANTEC Proc 1995, 2275.
21. K. J Kim, White, J. L. Polym Eng Sci 1999, 39, 2189.
22. Wang, Y.; Yu, M.-J. Polym Comp 2000, 21, 1.
23. Einstein, A. Ann Phys 1906, 19, 289.
24. Einstein, A. Ann Phys 1911, 34, 591.
25. Li, L.; Masuda, T. Polym Eng Sci 1990, 30, 841.
26. Supaphol, P.; Lin, J.-S. Polymer 2001, 42, 9617.
27. Supaphol, P.; Spruiell, J. E. Polymer 2001, 42, 699.